第 50 卷 第 16 期/2023 年 8 月/中国激光 研究论文

中国激光

激光增材连接TA15钛合金显微组织及力学性能研究

牟建伟[1]，于传军[1]，汤海波[2]，张述泉[2]，朱言言[2]，田象军[2*]

[1]沈阳飞机工业（集团）有限公司，辽宁 沈阳 110031；

[2]北京航空航天大学大型金属构件增材制造国家工程实验室，北京 100191

摘要 针对某大型复杂整体钛合金构件的激光增材制造，开展了激光增材连接TA15钛合金结构样件的制备，分析了整个结合区的组织及力学性能。结果表明：激光增材连接TA15钛合金结合区的冶金质量良好，连接区的凝固组织是从母材本体外延生长的粗大β柱状晶，显微组织是与母材本体基本相同的超细α+β网篮组织。从低倍照片中可观察到连接区与母材本体的分界线，但高倍金相照片中表面分界线两侧钛合金的显微组织无明显差异。对结合区不同方向的室温拉伸、室温冲击和室温断裂韧度性能进行了测试，并与母材本体的相应性能进行了对比，发现激光增材连接TA15钛合金结合区的力学性能可达到母材本体性能的100%，结合区横向的室温抗拉强度、伸长率、冲击韧性和断裂韧性分别为1046 MPa、7.2%、33.17 J/cm^{2}和78.2 MPa•m$^{1/2}$。该结果表明激光增材连接工艺可用于大型整体钛合金构件的高性能制造。

关键词 激光技术；激光增材连接；激光增材制造；显微组织；力学性能；钛合金

中图分类号 TG146.2 **文献标志码** A **DOI:** 10.3788/CJL221345

1 引 言

高性能大型钛合金构件的激光增材制造是以钛合金粉末为原料，通过激光熔化/快速凝固逐层沉积“生长制造”，利用计算机辅助设计(CAD)模型一步完成全致密、高性能大型整体钛合金零件的“近净成形”。与传统制造技术相比，激光增材制造技术无需大型锻造工业装备，具有制造周期短、材料利用率高、生产成本低等优势，构件组织细小均匀且综合力学性能优异，受零件尺寸和复杂程度的约束小，对构件设计变化有“超常”的快速响应能力，尤其适用于制造航空航天领域中的大型复杂整体钛合金结构件，是国内外研究热点[1-5]。随着飞机性能的不断提升和结构的不断优化，人们对大型复杂整体零件的需求越来越大，这对激光增材制造技术提出了严峻的挑战[6-7]。在三维大规格结构的“铸锭+锻造+机加”传统工艺中，坯料冶金质量及其一致均匀性难以保障。激光增材制造技术是该高效能整体结构的有效制造技术途径[8-9]。

零件尺寸和复杂程度的增加一方面要求激光增材制造成套设备的成形腔尺寸和运动机构能力不断增加；另一方面大型/超大型零件整体成形时变形开裂的潜在风险很大，后续热处理过程中零件的变形控制也非常困难，零件容易变形、开裂甚至报废[2]。首先对大型复杂整体零件进行分段激光增材制造，然后采用激光增材连接将其连接成整体结构，这样不仅可以降低激光增材制造对设备的要求和依赖，减小成形腔尺寸，降低制造成本，同时也可显著降低大型构件增材制造及后处理过程中的变形开裂控制难度。基于激光增材制造工艺实现两部分或多部分高性能金属构件的连接成形的技术称为激光增材连接，而连接区域称为激光增材连接区。

激光增材连接技术基于激光增材制造技术，通过对连接区域进行离散化的逐层熔化沉积，实现零件的全致密冶金熔合连接[5,10-12]。相较于传统焊接连接技术，激光增材连接技术具有独特的技术优势：1)逐层熔化能量输入小，连接区凝固组织细小，力学性能优异；2)低能量、小热量的离散输入，有效减少了激光增材连接过程对基材的热影响；3)小熔池的逐层熔化沉积-快速凝固可有效避免气孔、疏松、偏析等缺陷形成，实现对缺陷尺度的主动控制；4)受构件连接部位尺寸和结构形式的影响相对较小，工艺灵活，设备相对简单；5)激光增材连接过程受控，连接质量一致性与稳定性高[2,13-14]。

激光增材制造钛合金的微观组织及力学性能已有大量报道，人们对影响其服役性能的因素也已有了较为充分的认识[15-20]，但激光增材连接技术的报道较少，关于激光增材连接区及热影响区的微观组织及力学性能尚缺乏研究和认识。基于此，本文以TA15钛合金为研究对象，开展了激光增材连接TA15钛合金构件连接区显微组织形态的研究，对连接区力学性能进行

收稿日期：2022-10-20；**修回日期**：2022-12-04；**录用日期**：2022-12-06；**网络首发日期**：2022-12-16

通信作者：*tianxj@buaa.edu.cn

了测试分析。

2 试验及方法

2.1 原材料及激光增材连接工艺

本文所用激光增材制造及激光增材连接TA15钛合金原材料均为旋转电极雾化法制备的球形粉末。激光增材制造和激光增材连接试验在北京航空航天大学大型金属构件增材制造国家工程实验室自主研发的激光定向能量沉积增材制造工程化成套装备上完成，关键工艺参数为：激光功率为7～8 kW、扫描速度为600～1000 mm/min、送粉速率为0.8～1.2 kg/h，熔化沉积增材制造过程在氩气气氛中进行，氧含量(体积分数)控制在80×10^{-6}以下。

激光增材连接TA15钛合金样件成形工艺示意图如图1所示。在激光连接成形过程中，首先采用成熟的激光增材制造钛合金成形工艺制备出激光增材制造TA15钛合金母材本体，张群莉等[21]的研究结果表明：预制坡的角度会对激光增材连接试样的力学性能产生一定的影响。本文采用的预制坡口的角度及尺寸如图1所示，在母材本体上预制完坡口后，再利用激光增材制造技术对坡口进行增材制造填充，完成激光增材连接TA15钛合金样件的制备，其中母材本体的沉积增高方向与连接区的沉积增高方向相同。因为激光增材连接TA15钛合金样件包含几个不同的区域，为了便于后续的描述及区分，将试样中同时包含连接区、母材本体区及二者中间的部分统一称为结合区。在激光增材连接后采用与激光增材制造TA15钛合金母材本体相同的普通退火热处理工艺：750 ℃保温2 h，空冷。如表1所示，本试验制备的激光增材连接TA15样件的母材本体和连接区化学成分与TA15钛合金粉末原材料无明显差异，说明成形工艺过程控制良好。

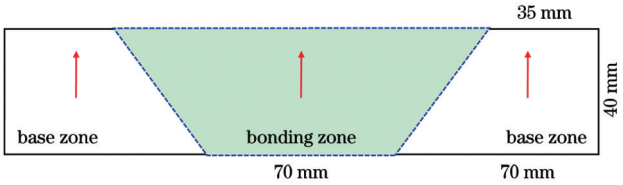

图1 激光增材连接TA15钛合金样件成形工艺示意图(箭头为沉积增高方向)

Fig. 1 Forming process diagram of TA15 titanium alloy samples by laser additive connection (arrows indicate deposition direction)

表1 TA15钛合金粉末和激光增材连接TA15样件的化学成分(质量分数，%)

Table1 Chemical compositions of TA15 titanium alloy powders and TA15 samples formed by laser additive connection (mass fraction, %)

Material	Ti	Al	Mo	V	Zr	Fe	C	N	H	O
Powder	Bal.	6.6400	1.5400	2.0400	2.1100	0.0500	0.0130	0.0120	0.0024	0.1100
Base zone of TA15 samples	Bal.	6.5900	1.6400	2.1000	2.1400	0.0280	0.0130	0.0120	<0.0010	0.1300
Connection zone of TA15 samples	Bal.	6.4600	1.6200	2.0700	2.1000	0.0380	0.0150	0.0140	0.0027	0.1200

2.2 试验方法

利用电火花线切割机从激光增材连接TA15钛合金样件上切取组织观察试样，取样方式和位置如图2所示，其中T向与增材逐层增高方向垂直(对应试样记为T向试样)，L向与增材逐层增高方向平行。切取的试样表面用水砂纸打磨，利用金刚石研磨膏抛光，并在HF、HNO_3、H_2O体积比为1∶6∶43的Kroll试剂中腐蚀10 s，利用光学显微镜(OM)和扫描电子显微镜(SEM)进行显微组织观察。

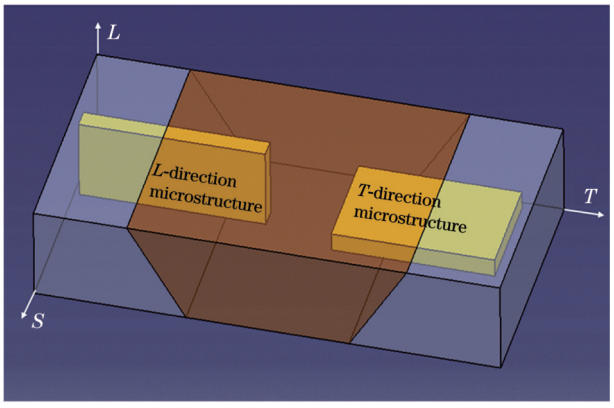

图2 激光增材连接TA15钛合金试样连接区取样示意图

Fig. 2 Sampling diagram in connection area of TA15 titanium alloy sample formed by laser additive connection

激光增材连接TA15钛合金的室温拉伸测试取样方式如图3所示，取样方向均为T向，采用棒状试样，测试6根平行试样并取平均值。室温冲击测试取样方式如图4所示，取样方向为T向，采取了两种开口方式，其中，开口平行于界面的冲击试样记为T-I开口试样，垂直于界面的记为T-II开口试样，采用55 mm×10 mm×10 mm的U型缺口冲击试样，测试3根平行

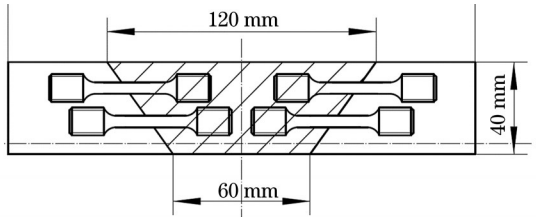

图3 室温拉伸测试中的取样示意图

Fig. 3 Sampling diagram in tensile test at room temperature

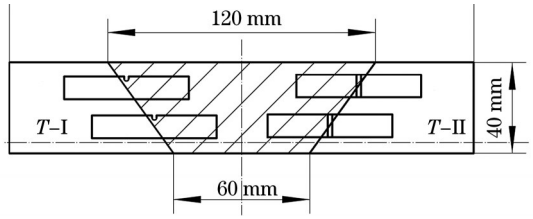

图 4 室温冲击测试中的取样示意图

Fig. 4 Sampling diagram in impact test at room temperature

试样并取平均值。室温断裂韧性测试取样方式如图 5 所示，采用厚度为 25 mm 的平面应变紧凑拉伸（CT）试样，测试 3 根平行试样并取平均值。当应力方向为图 2 所示 S 方向时，裂纹扩展方向为 T 方向，此时厚度中心位置的裂纹尖端开在结合区界面处，试样记为 ST 试样；当应力方向为 T 方向时，裂纹扩展方向为 S 方向，此时裂纹尖端的一半在连接区、一半在母材本体区，试样记为 TS 试样。

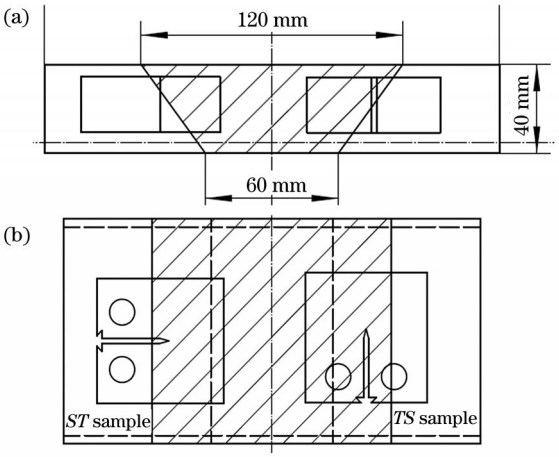

图 5 室温断裂韧性测试中的取样示意图。(a)正视图；(b)俯视图

Fig. 5 Sampling diagram in fracture toughness test at room temperature. (a) Front view; (b) top view

3 分析与讨论

3.1 激光增材连接 TA15 钛合金结合区的组织形貌

激光增材连接 TA15 钛合金结合区的横截面和纵截面低倍组织照片如图 6 所示。可以看出：在纵截面和横截面的低倍组织中，连接区与母材本体之间有一条明显的分界面，但界面两侧晶粒形貌和晶粒尺寸基本相同，界面处的衬度差异可能是由于连接区和母材经历的具体热影响历史不同。由纵截面组织可知：与母材本体相似，连接区的原始 β 晶粒也是沿着沉积增高方向从界面处母材本体的 β 柱状晶直接外延生长形成的，呈现出粗大的柱状晶组织。由于界面处的最大散热方向变化，连接区与母材分界面处的晶粒向着连接区略微倾斜，但这两个区域的晶粒尺寸也就是柱状晶的宽度相同。连接区的中间部分与母材本体无直接接触，β 柱状晶则从底部平行于沉积增高方向逐层外

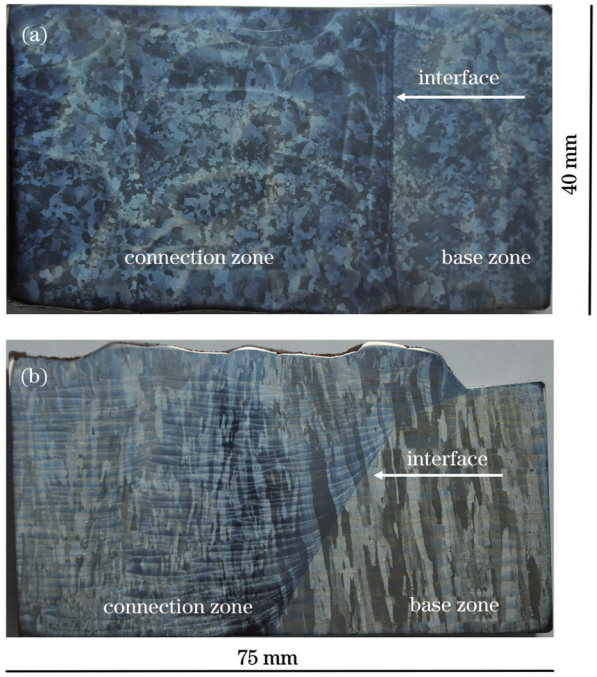

图 6 激光增材连接 TA15 钛合金试样结合区的低倍组织图。(a) T 向，横截面；(b) L 向，纵截面

Fig. 6 Low magnification microstructures of binding zone of TA15 titanium alloy sample formed by laser additive connection. (a) T-direction, cross section; (b) L-direction, longitudinal section

延生长，该区域的 β 柱状晶宽度略低于母材本体。在横截面上，连接区和母材本体的晶粒形貌均呈等轴状，本质上为外延生长的粗大 β 柱状晶的横截面形貌；连接区与母材本体的晶粒尺寸基本相同，可见激光增材连接过程对热影响区母材本体的晶粒形貌未产生影响，说明激光增材制造 TA15 钛合金原始 β 晶粒具有优异的热稳定性。

激光增材连接 TA15 钛合金纵截面不同区域的显微组织如图 7 所示，连接区（焊缝区）、界面区和母材的显微组织均是超细 α+β 细片层网篮组织。连接区的平均 α 片层厚度为 (0.96±0.13) μm，略低于母材本体的 (1.05±0.18) μm，如图 8 所示。这种轻微的差异主要是由于在激光增材连接过程中，连接区可以向两侧较大的母材本体散热，因而冷却速率略快。在界面附近的母材本体上没有观察到明显的热影响区，甚至在高倍条件下无法从显微组织中分辨出母材本体和连接区之间的界面。由于激光增材制造 TA15 钛合金母材及连接区采用了相同的原材料和制造工艺参数，其在沉积过程中经历的热历史基本一致，再加上相同的普通退火热处理制度，因此最终不同区域的显微组织基本相同。该结果再一次表明：对激光增材制造的 TA15 钛合金母材本体进行激光增材连接时，母材本体中不会形成明显的晶粒长大或显微组织粗化的热影响区，因而母材本体及界面处的力学性能不会恶化。

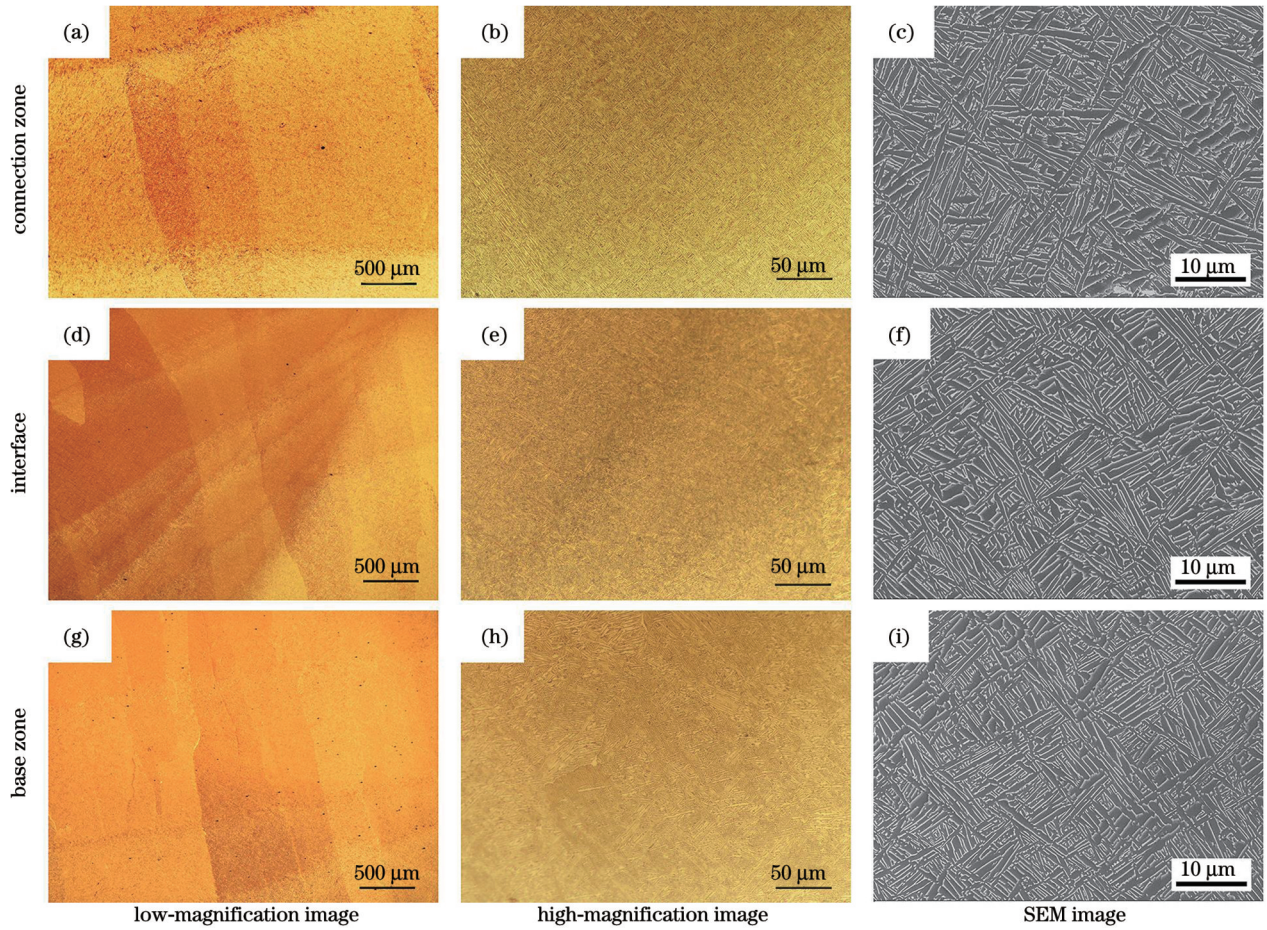

图 7 激光增材连接 TA15 试样纵截面不同区域的形貌

Fig. 7 Morphologies of different regions in longitudinal section of TA15 sample formed by laser additive connection

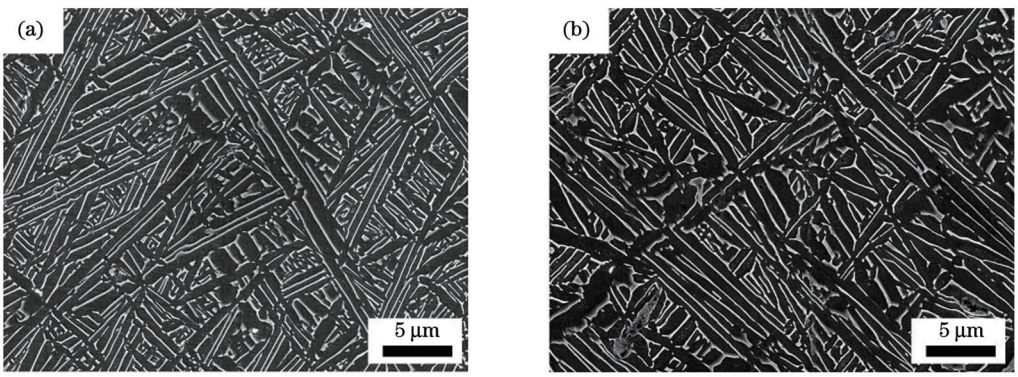

图 8 激光增材连接 TA15 试样横截面不同区域的 SEM 图。(a)连接区;(b)本体区

Fig. 8 SEM images of different regions in cross section of TA15 sample formed by laser additive connection. (a) Connection zone; (b) base zone

3.2 激光增材连接 TA15 钛合金构件的关键力学性能

激光增材连接 TA15 钛合金结合区的室温拉伸性能测试结果如表 2 所示,普通退火态结合区横向的抗拉强度和屈服强度分别为 1046 MPa 和 974 MPa,断后伸

表 2 激光增材连接 TA15 钛合金试样的室温拉伸性能

Table 2 Tensile properties of TA15 titanium alloy sample formed by laser additive connection at room temperature

Sampling position	Direction	Ultimate tensile strength /MPa	Yield strength /MPa	Elongation /%	Reduction in area /%
Bonding zone	*T*	1046	974	7.2	18.8
Base zone	*T*	1022	945	9.5	22.2
Forging standard	–	≥930	≥855	≥6	≥12

长率和断面伸缩率分别为7.2%和18.8%，均达到了TA15钛合金锻件标准水平。与增材制造母材本体普通退火态相比，结合区的室温拉伸强度略高、塑性略低，这种微小的差异可能与连接区更细的α片层宽度有关。从激光增材连接TA15钛合金结合区的室温拉伸结果可知：结合区室温拉伸试样的断裂位置随机出现在母材本体区和连接区。图9分别显示了在母材本体区与结合区断裂的拉伸试样断口形貌，二者断口均存在大量韧窝，显示出韧性断裂的特征。该结果表明：激光增材连接TA15钛合金的室温拉伸性能与激光增材制造母材本体基本相当，结合区内界面的存在对激光增材连接TA15钛合金室温拉伸力学性能没有明显影响。

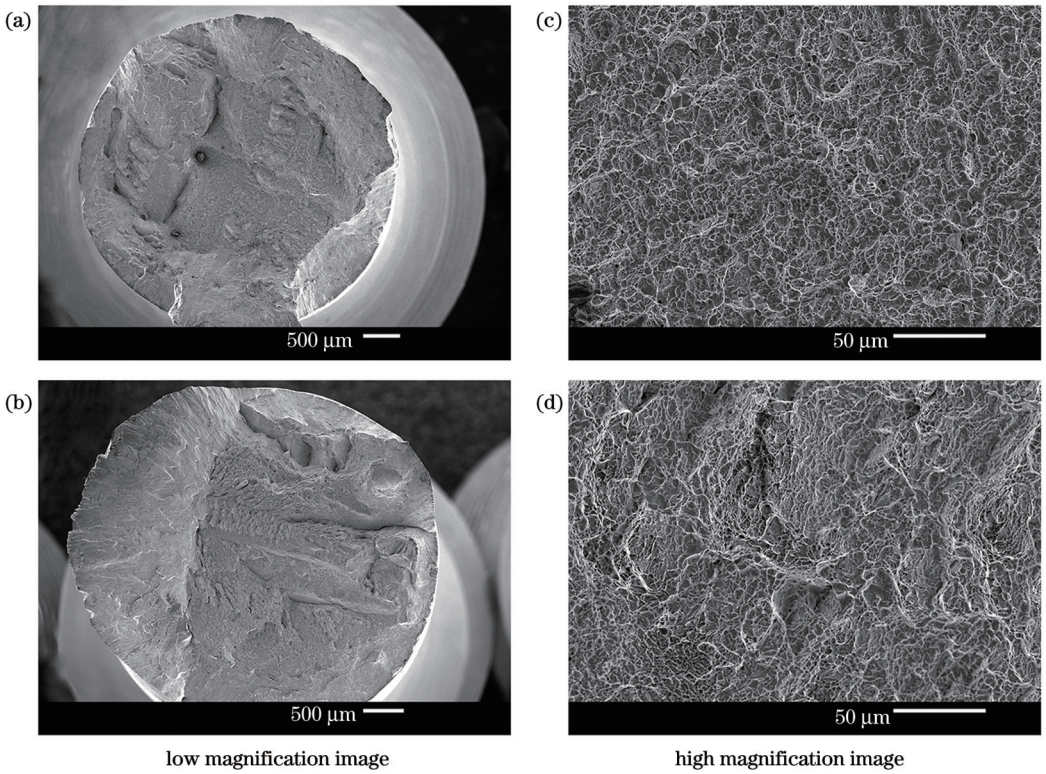

图9 激光增材连接TA15结合区的室温拉伸断口形貌。(a)(c)断裂位置在母材本体区；(b)(d)断裂位置在连接区

Fig. 9 Tensile fracture morphologies in binding zone of TA15 sample formed by laser additive connection at room temperature. (a)(c) Fracture at base zone; (b)(d) fracture at connection zone

激光增材连接TA15钛合金室温冲击韧性测试结果如表3所示，两种开口方式的结合区试样的室温冲击韧性分别为33.17 J/cm^{2}和33.96 J/cm^2，结合区冲击韧性无明显的各向异性。结合区室温冲击韧性与增材制造母材本体相当，该结果表明结合区界面的存在对激光增材连接TA15钛合金的室温冲击力学性能没有明显影响。

激光增材连接TA15钛合金结合区的室温断裂韧性测试结果如表4所示，结合区*ST*试样和*TS*试样的断裂韧性平均值分别为78.2 MPa·m$^{1/2}$和72.6 MPa·m$^{1/2}$，与*TS*试样母材本体的断裂韧性基本相当，断裂韧性性能较好。结合区*TS*试样的断口形貌如图10所示，本体区与结合区断口特征相似，均表现出韧性断裂特征，进一步表明激光增材连接TA15结合区和母材本体的断裂韧性无明显差异。优异的断裂韧性也保证了激光增材连接TA15钛合金大型整体构件的服役安全性。

表3 激光增材连接TA15试样的室温冲击性能

Table 3 Impact properties of TA15 sample formed by laser additive connection at room temperature

Sampling position	Sample	Impact toughness /(J·cm^{-2})
Bonding zone	*T*-I sample	33.96
	T-II sample	33.17
Base zone	*T* sample	31.60

表4 激光增材连接TA15的断裂韧性

Table 4 Fracture toughness of TA15 sample formed by laser additive connection

Sampling position	Sample	Average of fracture toughness /(MPa·m$^{1/2}$)
Bonding zone	*ST* sample	78.2
	TS sample	72.6
Base zone	*TS* sample	67.9

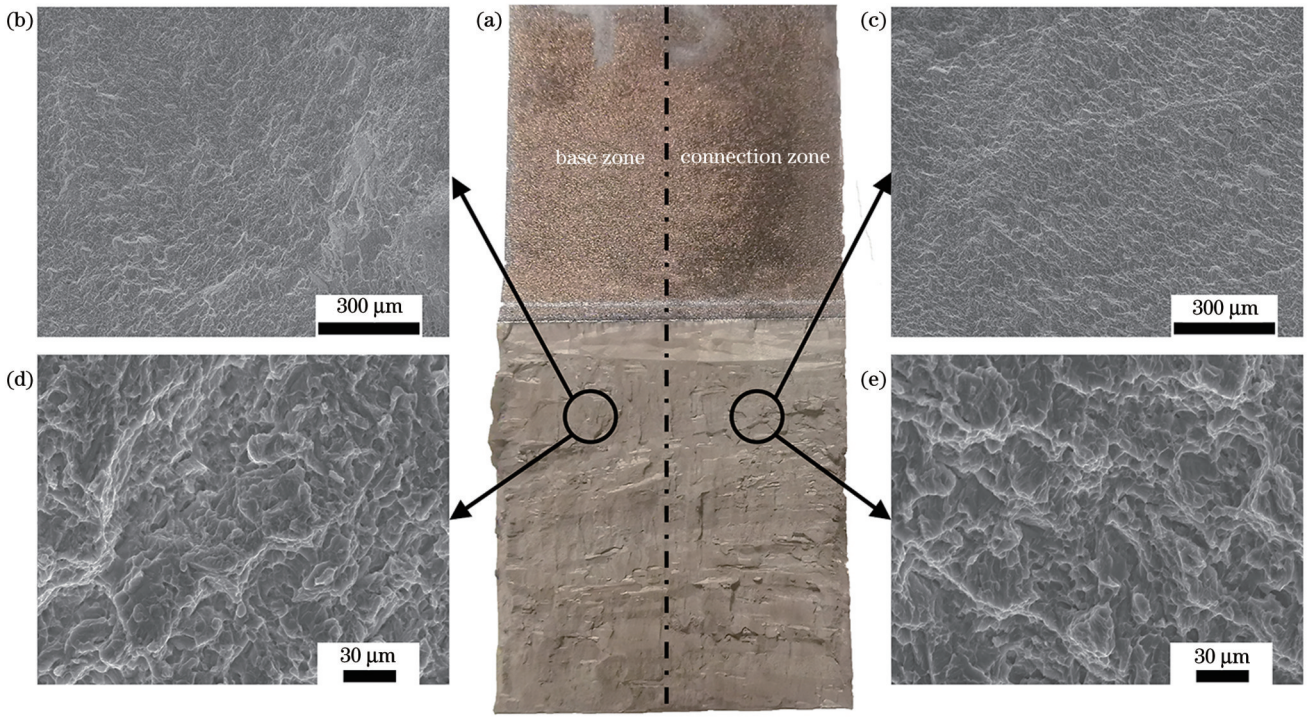

图 10 激光增材连接 TA15 结合区在室温断裂韧性测试中的断口形貌。(a)宏观断口形貌;(b)(c)低倍放大图;(d)(e)高倍放大图

Fig. 10 Fracture morphologies in bonding zone of TA15 sample formed by laser additive connection in fracture toughness test at room temperature. (a) Macroscopic fracture morphology; (b)(c) low magnification images; (d)(e) high magnification images

4 结 论

针对激光增材连接 TA15 钛合金样件开展了研究,对比了结合区不同位置处的显微组织,测试了结合区室温拉伸、冲击和断裂韧性性能,得到的结论如下:

1) 激光增材连接 TA15 钛合金的连接区为外延生长的粗大 β 柱状晶和晶内超细网篮 α+β 片层组织,显微组织形貌和尺寸与母材本体无明显差异,界面处无明显热影响区存在。

2) 激光增材连接 TA15 钛合金结合区的室温拉伸、冲击和断裂韧性性能与母材基本相当,结合区界面的存在对激光增材连接 TA15 钛合金的力学性能没有明显影响。结合区横向的室温抗拉强度、伸长率、冲击韧性和断裂韧性分别为 1046 MPa、7.2%、33.17 J/cm^2 和 78.2 MPa·m$^{1/2}$,达到了 TA15 钛合金锻件标准。该结果表明激光增材连接工艺可用于大型整体钛合金构件的高性能制造。

参 考 文 献

[1] 王华明, 张述泉, 王向明. 大型钛合金结构件激光直接制造的进展与挑战(邀请论文)[J]. 中国激光, 2009, 36(12): 3204-3209.
Wang H M, Zhang S Q, Wang X M. Progress and challenges of laser direct manufacturing of large titanium structural components (invited paper)[J]. Chinese Journal of Lasers, 2009, 36(12): 3204-3209.

[2] 王华明. 高性能大型金属构件激光增材制造: 若干材料基础问题[J]. 航空学报, 2014, 35(10): 2690-2698.
Wang H M. Materials' fundamental issues of laser additive manufacturing for high-performance large metallic components[J]. Acta Aeronautica et Astronautica Sinica, 2014, 35(10): 2690-2698.

[3] Zhu Y Y, Li J, Tian X J, et al. Microstructure and mechanical properties of hybrid fabricated Ti-6.5Al-3.5Mo-1.5Zr-0.3Si titanium alloy by laser additive manufacturing[J]. Materials Science and Engineering: A, 2014, 607: 427-434.

[4] Wolff S J, Lin S, Faierson E J, et al. A framework to link localized cooling and properties of directed energy deposition (DED)-processed Ti-6Al-4V[J]. Acta Materialia, 2017, 132: 106-117.

[5] 汤海波, 吴宇, 张述泉, 等. 高性能大型金属构件激光增材制造技术研究现状与发展趋势[J]. 精密成形工程, 2019, 11(4): 58-63.
Tang H B, Wu Y, Zhang S Q, et al. Research status and development trend of high performance large metallic components by laser additive manufacturing technique[J]. Journal of Netshape Forming Engineering, 2019, 11(4): 58-63.

[6] 顾冬冬, 张红梅, 陈洪宇, 等. 航空航天高性能金属材料构件激光增材制造[J]. 中国激光, 2020, 47(5): 0500002.
Gu D D, Zhang H M, Chen H Y, et al. Laser additive manufacturing of high-performance metallic aerospace components [J]. Chinese Journal of Lasers, 2020, 47(5): 0500002.

[7] 巩水利, 锁红波, 李怀学. 金属增材制造技术在航空领域的发展与应用[J]. 航空制造技术, 2013, 56(13): 66-71.
Gong S L, Suo H B, Li H X. Development and application of metal additive manufacturing technology[J]. Aeronautical Manufacturing Technology, 2013, 56(13): 66-71.

[8] Li Z, Cheng X, Li J H, et al. Thermal expansion properties of laser melting deposited Ti-6.5Al-2Zr-1Mo-1V alloy during α+β zone annealing[J]. Materials Characterization, 2017, 128: 115-122.

[9] 王华明, 张述泉, 王韬, 等. 激光增材制造高性能大型钛合金构件凝固晶粒形态及显微组织控制研究进展[J]. 西华大学学报(自然科学版), 2018, 37(4): 9-14.
Wang H M, Zhang S Q, Wang T, et al. Progress on solidification grain morphology and microstructure control of laser additively manufactured large titanium components[J]. Journal of Xihua University (Natural Science Edition), 2018, 37(4): 9-14.

[10] 胡悦, 刘莎莎, 程序, 等. 激光直接沉积 TA2/TA15 梯度材料弯

曲性能的有限元模拟[J]. 中国激光, 2020, 47(12): 1202006.
Hu Y, Liu S S, Cheng X, et al. Finite element simulation on bending properties of TA2/TA15 gradient material by laser direct deposition[J]. Chinese Journal of Lasers, 2020, 47(12): 1202006.

[11] Qian T T, Liu D, Tian X J, et al. Microstructure of TA2/TA15 graded structural material by laser additive manufacturing process [J]. Transactions of Nonferrous Metals Society of China, 2014, 24 (9): 2729-2736.

[12] 冯紫微, 周宝升, 张涛, 等. 铝合金与CF/PA66激光直接连接工艺及化学成键研究[J]. 中国激光, 2022, 49(13): 1303002.
Feng Z W, Zhou B S, Zhang T, et al. Investigation on laser direct joining of aluminum alloy-CF/PA66 and chemical bonding mechanism[J]. Chinese Journal of Lasers, 2022, 49(13): 1303002.

[13] Wang T, Zhu Y Y, Zhang S Q, et al. Grain morphology evolution behavior of titanium alloy components during laser melting deposition additive manufacturing[J]. Journal of Alloys and Compounds, 2015, 632: 505-513.

[14] Azarniya A, Colera X G, Mirzaali M J, et al. Additive manufacturing of Ti-6Al-4V parts through laser metal deposition (LMD): process, microstructure, and mechanical properties[J]. Journal of Alloys and Compounds, 2019, 804: 163-191.

[15] Li Z, Liu C M, Liu D, et al. Effect of heat treatment on microstructure and tensile properties of laser deposited titanium alloy TC21[J]. Materials Research Innovations, 2014, 18(sup4): S4-929.

[16] Zhu Y Y, Liu D, Tian X J, et al. Characterization of microstructure and mechanical properties of laser melting deposited Ti-6.5Al-3.5Mo-1.5Zr-0.3Si titanium alloy[J]. Materials & Design, 2014, 56: 445-453.

[17] Jiao Z G, Fu J, Li Z, et al. The spatial distribution of α phase in laser melting deposition additive manufactured Ti-10V-2Fe-3Al alloy[J]. Materials & Design, 2018, 154: 108-116.

[18] 袁红, 方艳丽, 王华明. 热处理对激光熔化沉积TA15钛合金组织及压缩性能的影响[J]. 红外与激光工程, 2010, 39(4): 746-750.
Yuan H, Fang Y L, Wang H M. Influence of heat treatment on microstructure and compressive property of laser melting deposited TA15 titanium alloy[J]. Infrared and Laser Engineering, 2010, 39 (4): 746-750.

[19] 刘炳森, 张述泉, 张纪奎, 等. 层间冷却对激光增材制造TC17钛合金组织和拉伸性能的影响[J]. 中国激光, 2022, 49(14): 1402204.
Liu B S, Zhang S Q, Zhang J K, et al. Effect of interlayer cooling on structure and tensile properties of TC17 titanium alloy fabricated by laser additive manufacturing[J]. Chinese Journal of Lasers, 2022, 49(14): 1402204.

[20] 姚讯杰, 王佳玮, 杨雁程, 等. 金属构件激光增材制造缺陷产生机理及控制机制探究[J]. 中国激光, 2022, 49(14): 1402802.
Yao X J, Wang J W, Yang Y C, et al. Review on defect formation mechanisms and control methods of metallic components during laser additive manufacturing[J]. Chinese Journal of Lasers, 2022, 49(14): 1402802.

[21] 张群莉, 李栋, 张杰, 等. 预制坡口角度对激光增材再制造IN718合金组织与性能的影响[J]. 表面技术, 2019, 48(5): 90-96.
Zhang Q L, Li D, Zhang J, et al. Influence of pre-fabricated groove angle on microstructure and properties of laser additive remanufactured IN718 alloy[J]. Surface Technology, 2019, 48(5): 90-96.

Microstructure and Mechanical Properties of TA15 Titanium Component Manufactured via Laser Additive Connection

Mou Jianwei[1], Yu Chuanjun[1], Tang Haibo[2], Zhang Shuquan[2], Zhu Yanyan[2], Tian Xiangjun[2*]

[1]*Shenyang Aircraft Industry (Group) Corporation Limited, Shenyang* 110031, *Liaoning, China*;

[2]*National Engineering Laboratory for Additive Manufacturing of Large Scale Metal Components, Beihang University, Beijing* 100191, *China*

Abstract

Objective Direct laser deposition (DLD) technology is a novel technique that directly fabricates full-density near-net-shape metal components from metal powders. During the DLD process, fine metal powders are fed into a molten pool produced by a sharply focused and high-energy laser beam. Compared to conventional techniques, the DLD process has some remarkable advantages: reduction of production cycle and cost, high material utilization ratio, and excellent flexibility. It has great potential for manufacturing large complex metal components, especially for difficult-to-process materials like titanium alloys. Therefore, it is suitable for preparing high-performance and large-scale titanium alloy components.

With the continuous improvement of aircraft performance requirements and the continuous optimization of the structure, the demand for large and complex integral parts is increasing steadily, which poses a severe challenge to DLD technology. On one hand, the forming cavity size and motion mechanism capacity of DLD equipment are required to increase continuously. On the other hand, as the size of the component increases, the component is prone to deformation, cracking and even scrapping during subsequent heat treatment. Therefore, the manufacturing method of using the DLD to connect different additive manufactured parts into a whole structure can address the aforementioned problems. The technology that involves forming two or more high-performance metal components by the DLD technology is called DLD connection, and the connection area is called DLD connection area.

DLD connection technology is based on the basic principle of the DLD process; that is, through the layer-by-layer melting deposition of the connecting area, the fully dense metallurgical fusion connection of the parts is achieved. It has many unique technical advantages, the most important of which is the microstructure of the DLD connection area is finer, and the mechanical properties are also excellent. The microstructure and mechanical properties of the DLD titanium alloy have been widely reported, and the factors affecting its service performance have been fully understood. However, there are few reports on DLD connection technology, especially concerning the research and understanding of the microstructure and mechanical properties of the DLD connection area and

the heat-affected zone. Therefore, this study takes TA15 titanium alloy as the research object and studies the microstructure of the DLD connection area of TA15 titanium alloy components by DLD connection technology. The mechanical properties of the DLD connection area also have been tested and analyzed.

Methods The raw TA15 powders used in the DLD and DLD connection processes are prepared by plasma rotating electrode processing. The DLD and DLD connection processes are carried out on the DLD engineering equipment under an argon atmosphere with oxygen volume fraction of less than 80×10^{-6}. The processing parameters are as follows: laser beam power of 7–8 kW, scanning speed of 600–1000 mm/min, powder delivery rate of 0.8–1.2 kg/h, and overlap ratio of 30%–50%. The forming process diagram of the DLD connection TA15 sample is shown in Fig. 1. First, the body area is prepared by the DLD process. Then the connection groove is prefabricated on the TA15 body. Finally, the DLD connection TA15 titanium alloy sample is completed until the groove is filled by the DLD technology. The deposition direction of the body area is the same as that of the DLD connection area. Table 1 presents the chemical compositions of the powder and the substrate materials. The microstructures of the samples corroded by Kroll reagent after polishing are observed by optical and scanning electron microscopes. Two samples, including the *T* and *L* direction samples perpendicular to the deposition direction, as illustrated in Fig. 2, are observed. Different mechanical properties, including room temperature tensile, room temperature impact, and fracture toughness properties, are also tested. The shape and dimensions of the different specimens are illustrated in Figs. 3–5.

Results and Discussions The microstructure of the DLD connection zone is the same as that of the additive manufactured base zone. The connection demarcation line can be observed in the low-magnification images. However, there is no obvious tissue difference between the two sides of the connection demarcation line in the high-magnification images. From the longitudinal section [Fig. 6(b)], the structure is similar to that of the base zone. On the cross-section [Fig. 6(a)], the grain morphologies of the DLD connection zone and the base zone are also equiaxed, and the grain sizes are the same. The microstructures of different regions in the DLD connection TA15 titanium alloy are shown in Fig. 7. The microstructures of these zones consist of an ultrafine $\alpha+\beta$ lamellar basketweave structure. We test the tensile, impact, and fracture toughness properties at room temperature in different directions of the bonding zone and compare them with the corresponding properties of the additive manufacturing base area. The existence of the DLD connection interface in the bonding zone exhibits no significant effect on the mechanical properties of the DLD connection TA15 titanium alloy. The tensile strength, elongation, impact toughness, and fracture toughness of the bonding zone at room temperature are 1046 MPa, 7.2%, 33.17 J/cm^2, and 78.2 MPa·m$^{1/2}$, respectively.

Conclusions Here, the microstructure and mechanical properties of the TA15 titanium components manufactured by DLD connection are investigated. The microstructures of different regions in the DLD connection zone and the base zone are the epitaxially grown β columnar crystal and ultrafine basket $\alpha+\beta$ lamellar structure within the β grains. The properties of tensile, impact, and fracture toughness at room temperature in different directions of the bonding zone are the same as those of the base zone. The existence of the DLD connection interface in the bonding zone has no obvious effect on the mechanical properties of the DLD connection TA15 titanium alloy. The tensile strength, elongation, impact toughness, and fracture toughness of the bonding zone at room temperature are 1046 MPa, 7.2%, 33.17 J/cm^2, and 78.2 MPa·m$^{1/2}$, respectively.

Key words laser technique; laser additive connection; laser additive manufacturing; microstructure; mechanical properties; titanium alloy